Computer Modeling of Crystalline Electrolytes: Lithium Thiophosphates and Phosphates

Nicholas Lepley and N.A.W. Holzwarth

Abstract

Recently, lithium thiophosphate materials suitable for usage as solid electrolytes in Li-ion battery applications have been developed. These materials possess room temperature ionic conductivities as high as 10^{-3} S/cm,[1] 3 orders of magnitude greater than that of commercial solid electrolyte materials based on LiPON.[2] The most promising of these thiophosphates, a superionic conductor with stoichiometry $Li_7P_3S_{11}$,[1] is investigated in this work using first principles calculations. In addition to examining the stability and structure of this material, we analyze in detail the migration mechanisms for both $Li_7P_3S_{11}$ and for hypothetical LiPON-like phosphate and phosphonitride analogues. Our results[3] correlate well with experimental findings and offer an explanation for the high conductivity observed in $Li_7P_3S_{11}$.

Overview

- Rechargeable batteries store charge in two electrodes that are separated by an electrolyte.
- During operation of the battery, the electrolyte transfers ions from one electrode to the other, while a corresponding amount of electrons flow through the external circuit.
- One of the most important properties for electrolyte materials therefore is ionic conductivity, which is given by the Arrhenius relation:
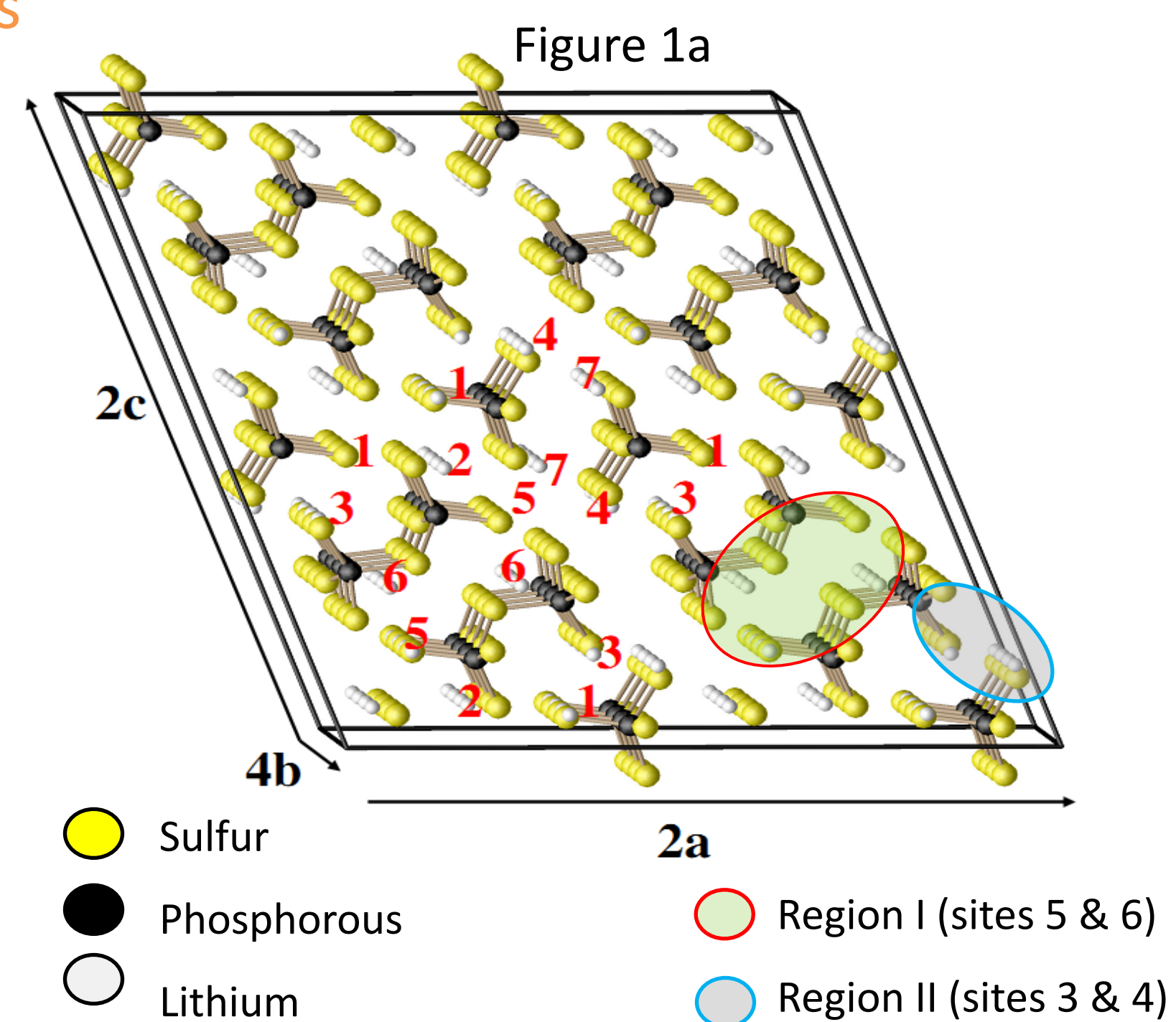
$$\sigma(T) = \frac{\sigma_0}{T} e^{-E_A/kT}$$

- In this equation T is temperature, k is the Boltzmann constant, σ_0 is a material dependent constant, and E_A is the activation energy.
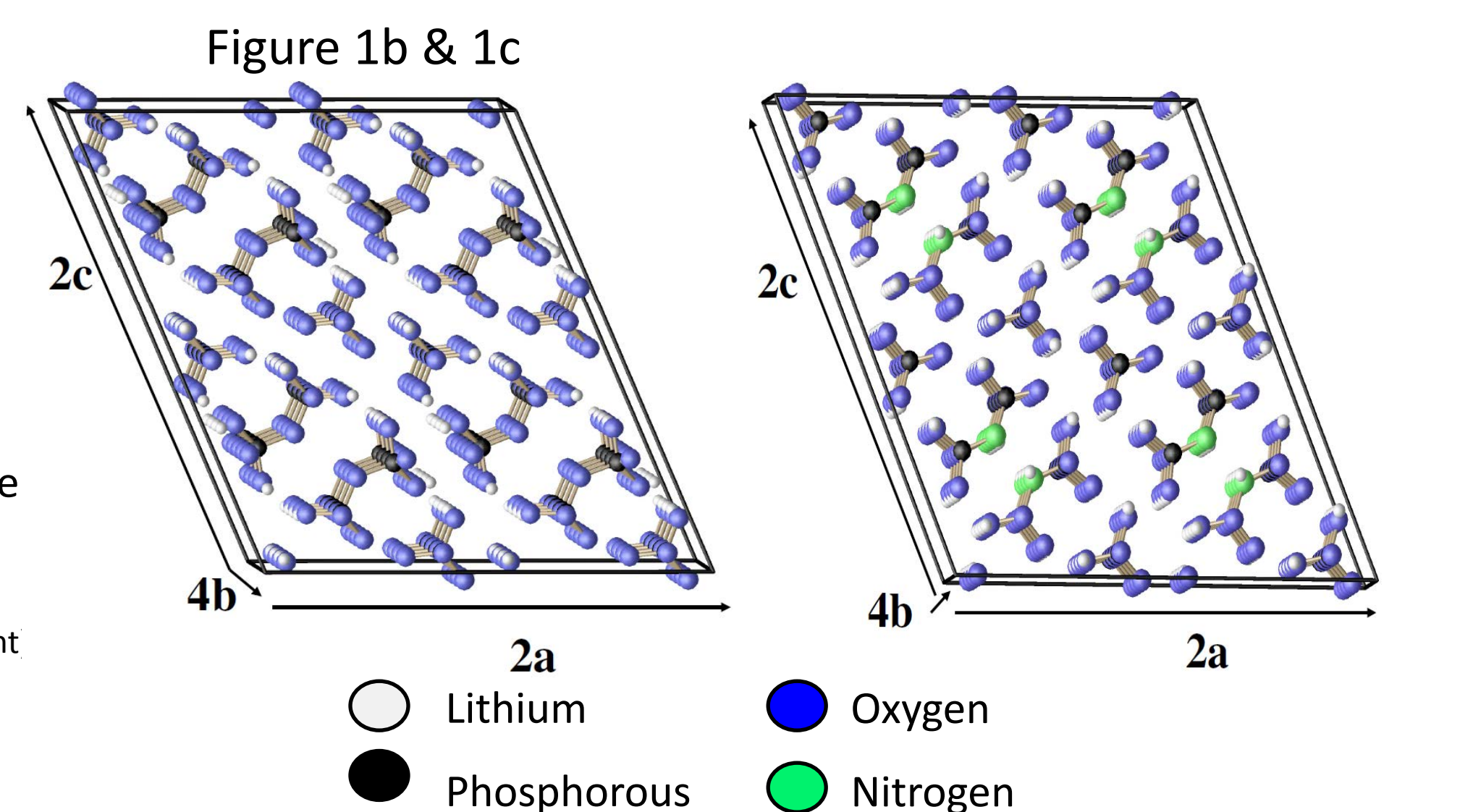
Materials

Figure 1a

$Li_7P_3S_{11}$ (Observed [1])
- 42 atoms per unit cell (2 formula units)
- $P\bar{1}$ symmetry
- $\therefore$ 7 inequivalent lithium positions
- Made up of P_2S_7 dimers and PS_4 tetrahedra
- Lithium often equidistant to multiple sulfur atoms, shared between tetrahedra and dimers
- Indicated regions are important for defect study (center)

- Sulfur (yellow)
- Phosphorous (black)
- Lithium (white)
- Region I (sites 5 & 6) (red circle)
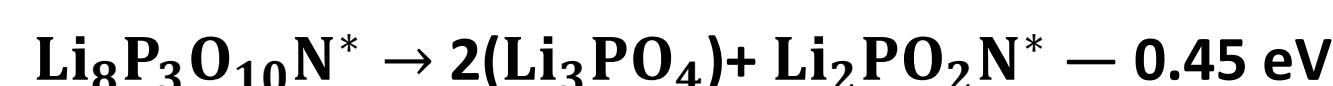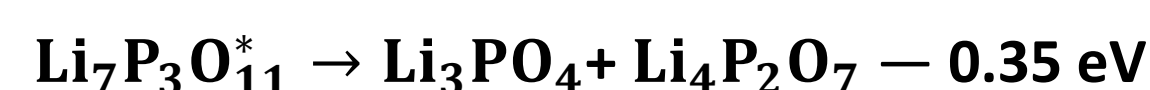- Region II (sites 3 & 4) (blue circle)

Figure 1b & 1c

Phosphate Analogues (Theoretical)
- By replacing S with O and N, metastable structures similar to $Li_7P_3S_{11}$ were found
- These structures were $Li_7P_3O_{11}^*$ and $Li_8P_3O_{10}N^*$
- Neither has been observed experimentally
- Provide possible insight into local structures in LiPON glass
- Facilitates comparison of phosphate and thiophosphate materials

(* denotes the structure has not been observed in experiment)

- Lithium (white)
- Phosphorous (black)
- Oxygen (blue)
- Nitrogen (green)

Computational Methods

General:
- Density functional theory (LDA)
- USPP and *pwscf*[4] (verified with PAW functionals generated using *atompaw,* and used in *pwscf* and *abinit*)
- Formation energies and perfect crystal properties:
  - $|k+G|^2 \leq 64$ bohr^{-2}
  - 3x6x3 k-point sampling
- Defect calculations:
  - 1x2x1 Supercell (approximately equal lattice vectors, ~84 atoms)
  - $|k+G|^2 \leq 32$ bohr^{-2}
  - 1x1x1 k-point sampling
  - Migration energies estimated using NEB method (E_m=energy range along path)
  - Extra electron added/removed for vacancy/interstitial calculations (and compensated with a uniform jellium of opposite sign) to accurately model mobile ions in insulating materials.

Specific:
- Interstitial site were identified using a grid-search algorithm
- Minimum-energy migration paths were determined via the construction of a weighted graph and the application of a shortest path algorithm.

Heats of Formation

Computation predicts all three materials to be unstable with respect to the listed decompositions into chemically stable forms.

$Li_7P_3S_{11} \rightarrow Li_3PS_4 + Li_4P_2S_6 + S$ — 0.78 eV

$Li_7P_3O_{11}^* \rightarrow Li_3PO_4 + Li_4P_2O_7$ — 0.35 eV

$Li_8P_3O_{10}N^* \rightarrow 2(Li_3PO_4) + Li_2PO_2N^*$ — 0.45 eV

Experimental observation confirms the metastability of $Li_7P_3S_{11}$ with respect to the thiophosphates used in the calculation above. While the $Li_7P_3S_{11}$ crystal is precipitated from a glass with high purity within the temperature range 280-360°C, and can then be quenched to room temperature, additional heating above 360°C results in the crystal breaking down exothermically into the Li_3PS_4, $Li_4P_2S_6$ mixture.[5]

Our results indicate that both $Li_7P_3O_{11}^*$ and $Li_8P_3O_{10}N^*$ are likely to decompose into more stable fragments.[6] To the best of our knowledge neither of these metastable crystal structures has been observed.

Defects

Vacancies (Fig. 1a)

- 7 unique Li vacancy sites (see Fig. 1a, left)
- Maximum energy difference between vacancy configurations ($E_4 - E_5$) is 0.28 eV.
- The lowest energy vacancy sites (most favorable to pure vacancy formation) are the sites 5 and 6 and are denoted Region I (Fig. 1a)
- The highest energy vacancy sites (least favorable to pure vacancy formation) include sites 1, 3,4 & 7 and a portion of this range is denoted Region II (Fig. 1a)

Interstitial Sites (Fig. 3)

- Several metastable interstitial sites can be identified (α to ζ by increasing energy).
- Maximum energy difference between interstitial configurations ($E_\zeta - E_\alpha$) is 0.19 eV.
- Many interstitial sites are in Region II, while none are in Region I (Fig. 3).

Regions

- Region I may be lithium saturated
  - ❖ Easy to form pure vacancy defects
  - ❖ Energetically expensive to form interstitial defects
- Region II may be lithium poor
  - ❖ Pure vacancy defects are energetically unfavorable
  - ❖ Easy to form interstitial defects

Vacancy-Interstitial Pair Formation (Fig. 3)

In addition to investigating each vacancy species separately, we explored the pair formation energy for pairs of defects. This is important because the experimentally measured activation energy E_A is defined by the formula:

$$E_A = E_m + \frac{E_f}{2}$$

Where E_f is the pair formation energy we will evaluate in this section, and E_m is the total barrier to migration across a unit cell, results for which are given in the next section of this poster.

- Several low energy vacancy-interstitial pairs (Frenkel Defects) are observed $Li_7P_3S_{11}$ (some of which are listed in Table I and visualized in Fig. 3).
- E_f for the pairs in the table is approximately zero.
- The negative value of E_f between native Li site 5 and interstitial site ε is likely due to the limited size of our supercell.

Phosphates
- E_f is the phosphate cases is approximately 0.8 eV for $Li_7P_3O_{11}^*$ and 1.2 eV for $Li_8P_3O_{10}N^*$.
- These structures possess much fewer low energy interstitial sites
- The lack of interstitial sites and the high formation energy (E_f) contribute to the lower conductivity observed in these materials.

Migration Results:

$Li_7P_3S_{11}$:
- The minimum energy migration path along each of the three crystallographic directions is shown on the right
- This minimum energy path is along the b-axis.
- The minimum migration barrier E_m= 0.15 eV.
- Significant structure in the paths correlates with low energy metastable sites.
- These metastable sites play an important role in the migration mechanism.
- Migration between the 3 and 4 sites (Region II) is the most favorable.
- Migration between 5 and 6 (Region I) is highly unfavorable.

Phosphate Analogues (Theoretical)
$Li_7P_3O_{11}^*$:
  - ➤ E_m= 0.52 eV for a path along the b-axis.
$Li_8P_3O_{10}N^*$:
  - ➤ E_m= 0.60 eV for a path along the a & c axes.

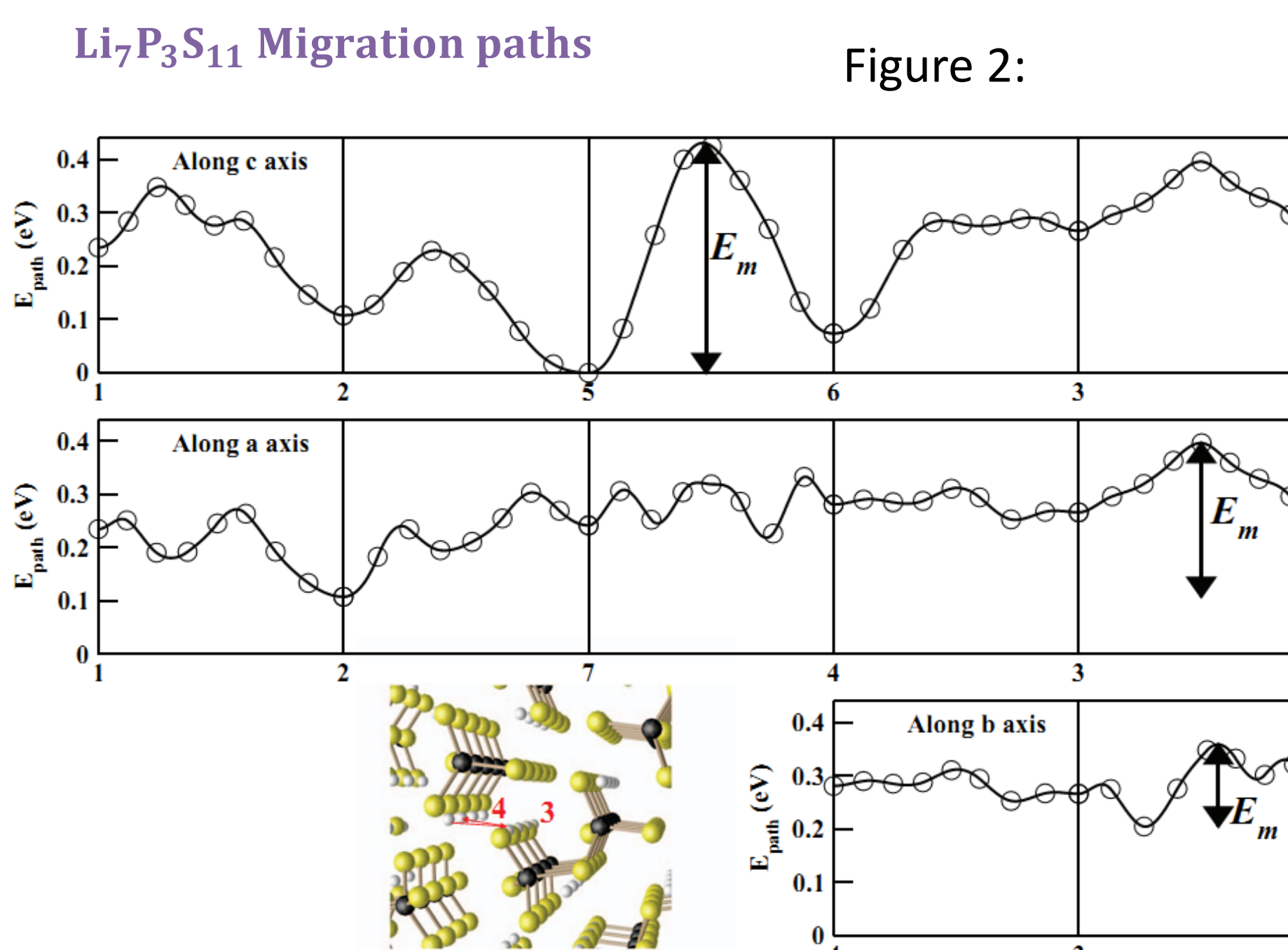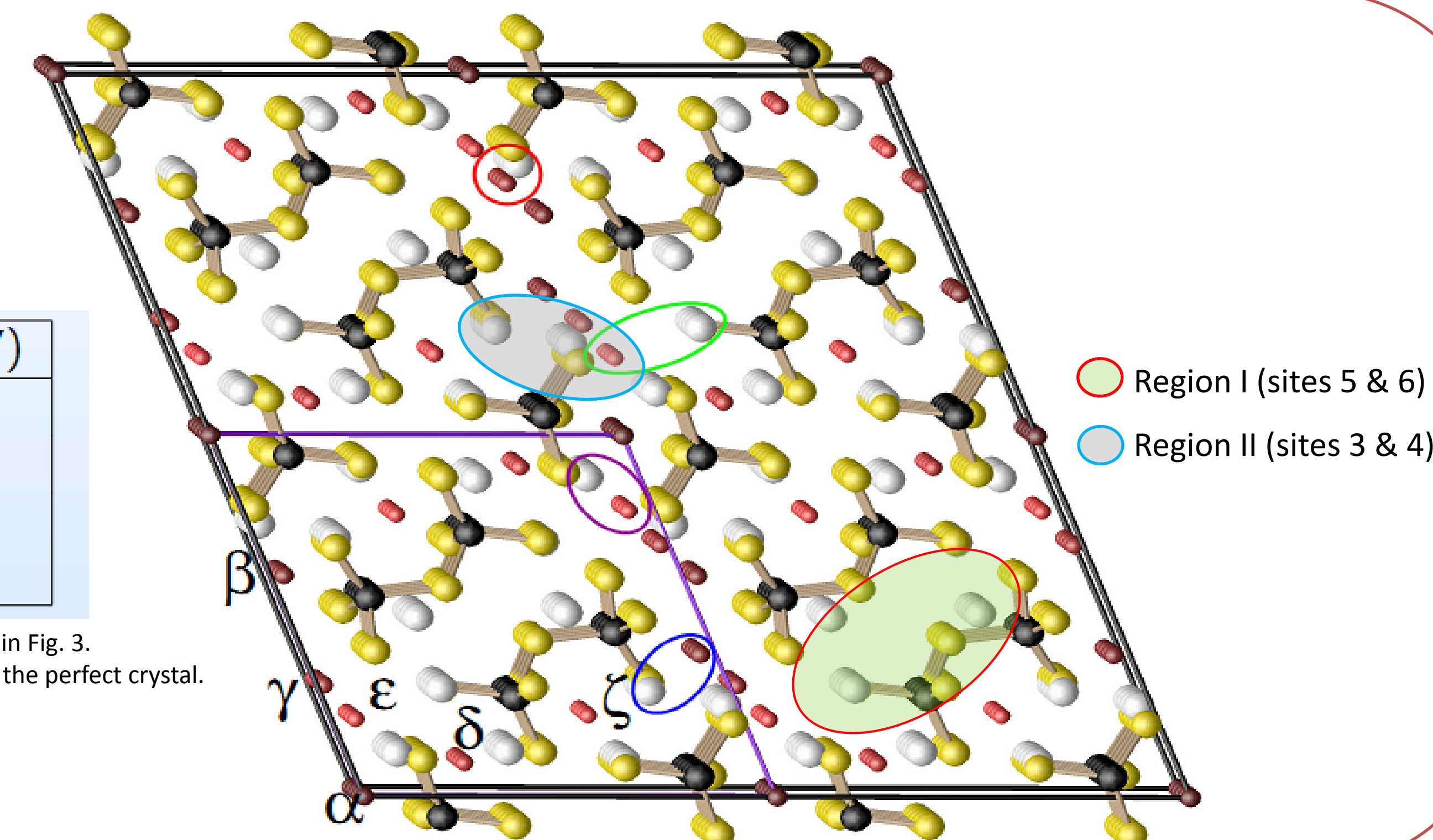- Both values are in approximate agreement with experimental results for related materials

$Li_7P_3S_{11}$ Migration paths

Figure 2:

Figure 3:

- Region I (sites 5 & 6)
- Region II (sites 3 & 4)

Table I

Label	E_f(eV)	E_{fm}(eV)
5ϵ	-0.03	0.13
4γ	0.02	0.08
3β	0.05	0.09
7ϵ	0.07	0.11

Table I: Colored labels in Table I correspond to circles in Fig. 3.
E_f is the energy of the defect configuration relative to the perfect crystal.
E_{fm} is the height of the barrier to defect formation.

Conclusions:

$Li_7P_3S_{11}$
- Modeled a metastable structure that approximately agrees with experiment with regard to formation energies, lattice vectors and atomic positions.
- Enthalpy of formation result confirmed experimental findings with regard to the metastability of $Li_7P_3S_{11}$.
- Migration energy E_m = 0.15 eV, while formation energy $E_f \sim 0$ yielding an activation energy of E_A =0.15 eV.
- Good agreement between calculated activation energy(E_A) and experimentally observed value (experimental E_A=0.12-0.18 eV[7]).
- A region with multiple metastable sites and low barriers to migration (Region II) and a region with no interstitial sites and high migration barriers (Region I) were identified.
- These regions approximately correspond to regions identified in experiment.[8]
- Low energy metastable sites that can be occupied by interstitial atoms or migrating vacancy atoms provide a mechanism for superionic conductivity in this material.

Phosphate Analogues
- Phosphate and phosphonitride migration barriers are significantly higher, but in line with experimental results for related materials.
- Phosphate and phosphonitride materials lack the low energy interstitial sites that are thought to contribute to high conductivity in the thiophosphate case.

References

1. F. Mizuno, A. Hayashi, K. Tadanga, and M. Tatsumisago, Solid State Ionics **177**, 2721 (2006).
2. N. J. Dudney, Interface **17**, 44 (2008).
3. N. D. Lepley and N. A. W. Holzwarth, Journal of the Electrochemical Society, **159**, A538-A547 (2012).
4. P. Giannozzi, S. Baroni, N. Bonini, M. Calandra, R. Car, C. Cavazzoni, D. Ceresoli, et al., J. Phys.: Condens. Matter, 21, 394402 (19pp) (2009), available from the website http://www.quantum-espresso.org.
5. K. Minami, A. Hayashi, and M. Tatsumisago, Journal of the Ceramic Society of Japan **118**, 305 (2010).
6. Y.A. Du, N.A.W. Holzwarth, Phys. Rev. B 81 (2010) 184106 (15 pp).
7. A. Hayashi, K. Minami, and M. Tatsumisago, Journal Solid State Electrochemistry **14**, 1761 (2010).
8. Y. Onodera, K. Mori, T. Otomo, A. C. Hannon, S. Kohara, K. Itoh, M. Sugiyama, and T. Fukunaga, J. Phys. Soc. Jpn. **79**, 87 (2010), suppl A; Proc. 3rd Int. Conf. Physics of Solid State Ionics (ICPSSI-3).